Eur Biophys J (2009) 38:1049–1059
DOI 10.1007/s00249-009-0507-0

ORIGINAL PAPER

# Probing the membrane potential of living cells by dielectric spectroscopy

**Corina Bot · C. Prodan**

Received: 17 April 2009 / Revised: 2 June 2009 / Accepted: 8 June 2009 / Published online: 5 July 2009


**Abstract** In this paper we demonstrate a quantitative way to measure the membrane potential of live cells by dielectric spectroscopy. We also show that the values of the membrane potential obtained using our technique are in good agreement with those obtained using traditional methods—voltage-sensitive dyes. The membrane potential is determined by fitting the experimental dielectric dispersion curves with the dispersion curves obtained from a theoretical model. Variations in the membrane potential were induced by modifying the concentration of potassium chloride in the solution of the cell suspension in the presence of valinomycin. For exemplification of the method, *E. coli* was chosen for our experiments.

**Keywords** *E. coli* · Cell suspension · Dielectric spectroscopy · Impedance analysis · Membrane potential · Voltage-sensitive dyes

**Abbreviations**

| | |
|---|---|
| *E. coli* | *Escherichia coli* |
| DS | Dielectric spectroscopy |
| IS | Impedance spectroscopy |
| OD | Optical density |

C. Bot · C. Prodan (✉)
Physics Department, New Jersey Institute of Technology, Tiernan Hall, 161 Warren Street, Newark, NJ 07102, USA
e-mail: cprodan@adm.njit.edu

C. Bot
e-mail: corina.bot@njit.edu

## Introduction

The resting membrane potential is one of the most important living-cell parameters. By monitoring a cell's membrane potential, one can get important information about its state. Changes in the membrane potential have been linked to different diseases, including Parkinson's, epilepsy, and Bartter's syndrome (Wright 2004). It was also shown that the membrane potential plays a critical role in the antibiotic uptake by cells and in bactericidal action (Mates et al. 1982). Thus, measuring or monitoring the membrane potential is of great importance. The standard methods to measure or monitor the membrane potential are patch-clamping and voltage-sensitive dyes. In patch-clamping, one measures the absolute value of the membrane potential, while with voltage-sensitive dyes one can only monitor changes in the membrane potential. Both methods are very effective, but they can be invasive or laborious.

Dielectric spectroscopy (DS) studies the complex dielectric function of the biological samples, which can be cells suspended in solution or tissues. Because it is noninvasive, this method is widely used in many areas including biophysics and pharmacology. For example, impedance spectroscopy (IS) has also been used to characterize the wound-healing process (Keese et al. 2004). Single-cell DNA content was determined using impedance monitoring (Sohn et al. 2000). In pharmacology, cellular dielectric spectroscopy has been used as a label-free technology for drug discovery (Leung et al. 2005). Researchers have quantified a detection time for *Salmonella typhimurium* and *Escherichia coli* (*E. coli*) O157:H7 cultures from the impedance growth curve (impedance against bacterial growth time) at 10 Hz (Yang and Li 2006). Also, rod-shaped cells (a *Streptomyces* strain with a filamentous

cellular shape) presented in a study (Ciureanu et al. 1997) were measured in the 10 Hz–13 MHz frequency range. Studies involving *E. coli* cells mainly showed the beta dispersion effects in the frequency range of 20 kHz–20 MHz (Zhivkov and Gyurova 2008), 75 kHz–20 MHz (Asami et al. 1999), and 1 kHz–110 MHz (Bai et al. 2007). The dielectric measurements of an *E. coli* cell suspension and liposome suspensions were carried out in the frequency range between 0.1 and 100 MHz to detect the heat-stress-mediated interaction between proteins and cell membranes (Morita et al. 2000). Dielectric measurements on mammalian cells were used as screening methods for cytoplasm- and membrane-specific markers in the frequency range 1 kHz–100 MHz (Ron et al. 2008).

It was previously shown that the presence of the membrane potential has a specific effect on the dielectric behavior of cell suspensions, namely the appearance of a frequency dependence called the α-dispersion, which is present in the low-frequency part of the dielectric dispersion curves (Prodan and Prodan 1999; Prodan et al. 2008). Thus, low-frequency dielectric spectroscopy could be developed into a label-free, fast, and noninvasive technique to measure or monitor the membrane potential and its changes. This represents the main purpose of this article. Here we demonstrate a quantitative way to measure the membrane potential of living cells by dielectric spectroscopy that is applicable to any type of live cell. We also show that the values of the membrane potential obtained using our technique are in good agreement with those obtained using traditional methods—voltage-sensitive dyes. For exemplification, our method was applied to *E. coli*.

The membrane potential of *E. coli* is determined by fitting the experimental dielectric dispersion curves with a theoretical model (Prodan and Prodan 1999; Prodan et al. 2008). Variations in the membrane potential were quantified using DS and the traditional method of voltage-sensitive dyes. These changes were induced by modifying the concentration of KCl in the solution in the presence of valinomycin. Cells were prepared in the same way for both types of experiments. For DS, we applied a recently introduced method to remove the electrode polarization error from the live-cell suspension dispersion curves (Prodan and Bot 2009).

## Materials and methods

*Escherichia coli* K12 wild type (ATCC) were incubated in 5 ml of Tryptone Soy broth (growth medium) at 175 rpm and 37°C to saturation phase for 16 h. For cell viability in water, the culture was then re-suspended in 60 ml of medium and incubated in the same conditions to a mid-logarithmic phase for 4 h. For DS, cells were incubated 12 h in three test tubes, each with 5 ml of Tryptone Soy broth, then mixed together. After reaching saturation phase, 2 ml of cells were re-suspended in 23 ml of medium and incubated in the same conditions to a mid-logarithmic phase for 2.5 h to an OD of 0.615.

For cell viability in water, two test tubes with 10 ml of cells in medium and cells in autoclaved DI water were tested for 7 days. Each day, cells were cultivated on agar plates by serial dilutions and incubated for 18 h at 37°C and the number of colonies counted from the $10^{-7}$ area. In parallel, a test tube with cells in medium was kept in the same conditions. Daily, a serial dilution was performed, and plates were inoculated for each cell concentration. Cells were imaged at 100× magnification, and images were taken with a CCD camera (Sensicam, The Cooke Corporation) attached to a Zeiss Axiovert 200 inverted microscope.

Fluorescence measurements were performed on cells harvested and re-suspended under the same conditions as for DS, with a Varian–Cary Eclipse Spectrophotometer. The voltage-sensitive dye used for staining the cell membrane was Di-$SC_3$-5 carbocyanine iodide (AnaSpec) with an excitation wavelength of 642 nm and emission wavelength 670 nm. Dye was added at a concentration of 0.4 μM (Wu et al. 1999) both to cells in medium and cells in water. All fluorescence measurements were performed after a cell incubation of 15 min to allow the dye to settle in the membrane.

Dielectric spectroscopy measurements were performed with a Two-Channel Dynamic Signal Analyzer SR785 over the frequency range 10 Hz–100 kHz and with a Solartron 1260 Impedance Analyzer over the frequency range 10 Hz–1 MHz. We used the same experimental setup as previously described in Prodan et al. (2004). The cell suspension to be measured is placed between two parallel gold-plated electrodes that are enclosed in a cylindrical glass tube. In order to minimize the chemical reactions between the electrodes and the solution, gold, an inert metal, was plated on the electrodes. The electrodes can be easily replaced with new ones if they deteriorate. The set up was previously reported to measure accurately the dielectric permittivity of different liquids with known dielectric permittivity from 4 to 78 (water) (Prodan et al. 2004). The guard electrode technique for reducing the stray effects was also tested. Results reported here were obtained with electrodes of 28.1 mm in radius. The distance between the electrode plates was 3 mm, and the applied electric field was 1 V/cm. The set-up provides the complex impedance $Z$ of the measuring cell over the frequency ranges mentioned above. The cleaning procedure was washing with water for 1 min followed by a three times rinse with DI water for both the chamber and the

electrodes. Before and after a measurement set, DI water was re-measured. This routine is very satisfactory since the water measurements after the washing gave highly reproducible results.

For DS, a fresh suspension of cells was centrifuged at 2,522×$g$ for 6 min before each measurement and the pellet re-suspended in ultrapure water (from a Milli-Q Direct Q) with 5 mM glucose to the desired $OD_{600}$. Glucose was used to balance the osmotic pressure.

A major source of error when measuring the impedance of liquid samples is the polarization that appears at the contacts between the sample and electrodes (Prodan et al. 2004). The superficial layer of charges near the electrodes polarizes when electric fields are applied, leading to the electrode polarization effect, which is predominant at low frequencies. There are several methods for removing the polarization error (Bordi et al. 2001; Raicu et al. 1998; Schwan 1968). We chose the one presented in Prodan and Bot (2009) because it makes no assumption of the impedance of the electrode polarization, rather this impedance is measured experimentally. Moreover, this technique was shown to be in line with the one presented in Bordi et al. (2001) where the electrode polarization impedance was modeled as a power law. We should mention that this technique is applicable only to suspensions with low volume fraction. The measured impedance $Z$ is a sum of the intrinsic impedance of the sample, $Z_s$, and the impedance of the polarization layers, $Z_p$: $Z = Z_s + Z_p$. $Z_p$ is caused by the medium in which the cells are suspended rather than the cells themselves. Therefore, $Z_p$ can be obtained from measurements on the medium alone. Hence, after each DS measurement, the sample was centrifuged and the supernatant was collected. Extreme care was taken to minimize possible breaking of the cells. For the first set of measurements, cells were centrifuged at 2,522×$g$ and then supernatant was collected. The solution with cells at OD 0.206 was centrifuged for 10 min and then the supernatant was collected. For OD 0.434 and OD 0.638, cells were centrifuged 2 min, the supernatant was collected and then centrifuged again for 2 min. The same procedure was repeated for another 4 min. The DS measurements on the resulting supernatant (centrifuged 10 min total) were done under the same conditions as the cells. For the higher concentrations of cells (OD 0.4, 0.6), a much gentler centrifugation is required to avoid membrane breakage. The membrane breakage releases ions, increasing the conductivity of the supernatant. To be sure that the supernatant had the same ionic properties as the suspension medium during the DS measurements, high-frequency conductivity measurements were taken from the cell suspension and from the supernatant, making sure that the two values coincided.

Once the medium was separated, we eliminated $Z_p$ by applying the following steps.

1. Record the impedance of the medium, $Z_m$, for each frequency.
2. In the high-frequency range, where the polarization effect is absent, fit $Z_m$ with the ideal impedance given in Eq. 1 and use the dielectric permittivity $\varepsilon$ and conductivity $\sigma$ as fitting parameters:

$$Z_{ideal} = (x/A)/(j\omega\varepsilon + \sigma) \quad (1)$$

In this equation, $x$ represents the distance between the capacitor plates and $A$ their surface area.

3. Once the intrinsic $\varepsilon$ and $\sigma$ of the medium are obtained, use these values to extrapolate $Z_{ideal}$, which now represents the intrinsic impedance of the medium, all the way to zero frequency.
4. Compute $Z_p$ as the difference between $Z_m$ and the extrapolated $Z_{ideal}$.
5. Correct the impedance $Z$ by subtracting $Z_p$ calculated above and obtain the intrinsic impedance of the sample $Z_s$.

For fluorescence and DS, 1 μM valinomycin was added (Wu et al. 1999) to make the membrane permeable to $K^+$. Valinomycin was bought from Molecular Probes and hydrated in DMSO spectrophotometric grade, 99.9% (ACROS Organics), to a 2.2 mM stock concentration.

A theoretical model, showing that the membrane potential plays a dominant role in the low-frequency dielectric dispersion curves, was utilized to fit the experimental data to obtain the membrane potential (Prodan et al. 2008). The model is applicable in the 1 Hz–100 MHz frequency range and in the limit of small applied electric fields. The following gives a brief description of this model. Each cell in suspension is modeled as a composite dielectric body, made of a dielectric shell representing the membrane ($\varepsilon_1$, $\sigma_1$) and a dielectric core ($\varepsilon_2$, $\sigma_2$), with superficial charge distributions on the outer and inner faces of the membrane ($\rho_1$, $\rho_2$). These charges cannot leave the surface of the membrane, but they can move freely on it, generating singular currents. The shelled particles with surface-charge distributions are suspended in an electrolyte with ($\varepsilon_0$, $\sigma_0$).

(1) For this system, $\varepsilon^*(\omega) = \varepsilon_0(1 - [p\alpha(\omega)/(1 - p\alpha(\omega)/3)])$, where $p$ is the volume fraction of cells and $\alpha$ is the polarizability.

(2) The system of equations used to calculate $\alpha$ includes the Laplace equations for the electric potential, the continuity equations for the surface charges, and the boundary conditions at the surfaces of the membrane. The polarizability was found to depend on the

conductivity of the superficial charges, $\gamma_i$, among other parameters.

(3) The membrane potential $\Delta V$ is related to the conductivity of the superficial charges, $\gamma_i$, on the inner or outer surface of the membrane as $\Delta V = 3.00 \frac{\gamma_i}{D_i} \frac{d}{\varepsilon_1/\varepsilon_{vac}}$ with $d = R_2 - R_1$, thickness of the membrane in nanometers, and the rest of the parameters being expressed in international units.

Combining steps (1), (2), and (3), the solution for spherical cells in suspension is

$$\alpha(\omega) = \frac{6\lambda}{3-\lambda}\left[1 - \frac{\Delta V \frac{2R_2\varepsilon_1/\varepsilon_{vac}}{3d}}{\left(1+\frac{j\omega R_2^2}{2D}\right)(3-\lambda)\left(\varepsilon_{10}^* + \varepsilon_0^*\right) + \Delta V \frac{2R_2\varepsilon_1/\varepsilon_{vac}}{3d}}\right]$$

$$\text{with} \quad \lambda = \frac{\left(\varepsilon_2^* - \varepsilon_1^*\right)}{\left(\varepsilon_2^* + \varepsilon_1^*\right)}; \quad \varepsilon_{10}^* = \varepsilon_1^*\left\{1 - \frac{3}{1 - \left(\frac{R_1}{R_2}\right)^3 \frac{\varepsilon_2^* + 2\varepsilon_1^*}{\varepsilon_2^* - \varepsilon_1^*}}\right\}$$

where $D$ represents the diffusion coefficient.

Changes in the membrane potential have a dramatic influence in the alpha regions: the larger $\Delta V$, the stronger the alpha dispersion as seen in Fig. 1. Here $\Delta V$ is changed in 20-mV steps from 180 to 120 mV. Cell diameter is 3 μm, $\varepsilon_1 = 10$, $\sigma_0 = 0.002$ S/m, $\varepsilon_0 = 78$, $\varepsilon_2 = 80$, $\sigma_2 = 0.2$ S/m, and $d = 2$ nm. Also, the outer conductivity has a large effect on the beta dispersion. As $\sigma_0$ increases, so does the frequency where beta dispersion appears. If $\sigma_0$ becomes very small, the separation between alpha and beta mechanisms becomes undifferentiated. We should also note that in this theoretical model, the effect of electrorotation was not considered.

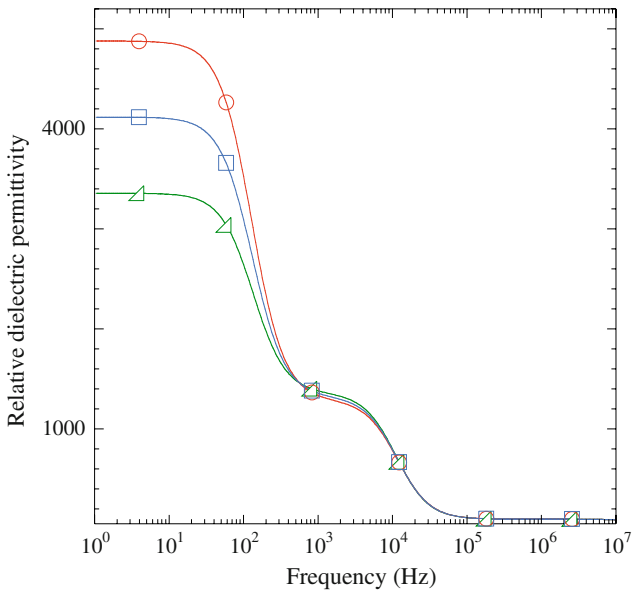


**Fig. 1** Dependence of membrane potential ($\Delta V$) on relative dielectric permittivity. Numerical values: $\Delta V = 180$ mV (*red*, *empty circle*), $\Delta V = 140$ mV (*blue*, *empty square*), $\Delta V = 120$ mV (*green*, *empty triangle*). As the membrane potential is increased from 120 to 180 mV, the low-frequency dielectric permittivity increases accordingly

## Results

In order to quantify the intrinsic response of the cells, it is desirable to have an electrode polarization effect as low as possible. Thus, one would like to consider a suspension fluid with a low ionic strength, and this motivated our choice for pure water with 5 mM glucose as suspension medium for the *E. coli*. Before the actual DS measurements, we tested the viability of the cells in sterile DI water over a period of 7 days as described in "Materials and methods." In Fig. 2 we present the results of this viability study. From each inoculated plate, the number of colonies from $10^{-7}$ dilution was counted and plotted versus time. In the first 100 h, we identified a slight growth followed by a regression; also, from 150 h on, the same pattern is followed. This slight growth is expected since some cells undergo apoptosis, breaking down, and releasing nutrients for the other living cells.

Next, we wanted to study how the cell membrane potential responds to the transition from growth medium to the suspending medium, water with glucose. We used the voltage-sensitive dyes method described in "Materials and methods." We observed that, when the cells were harvested from the growth medium and placed in water, their membrane potential changed. This is a direct result of their

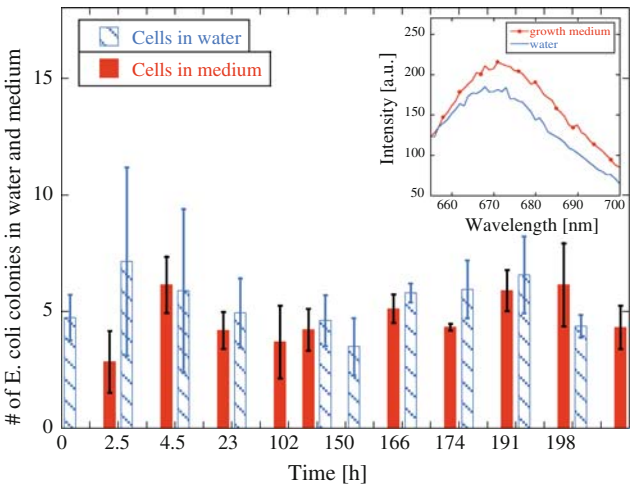


**Fig. 2** Number of *E. coli* colonies in water and medium counted from the $10^{-7}$ area of serial dilution versus time. *Red*, *solid columns* represent cells in media and *blue*, *dashed columns* cells in water. *Inset* represents fluorescence intensity changes versus wavelength for cells in medium (*red*, *solid circles*) and cells in water (*blue line*)

adaptability to the new conditions. Fluorescence intensity of cells in medium and cells in water (average of five measurements) is plotted versus wavelength in the inset in Fig. 2. The cells in water exhibited a decrease in fluorescence intensity, which is directly proportional to a decrease in membrane potential. Hyperpolarization occurs first due to a pH change and second due to a hyperpolarization of the cell membrane when $K^+$ diffuses outside to balance $\Delta V$ to equilibrium.

After these tests showing cells are viable in water with 5 mM glucose, we performed DS measurements at different cell concentrations (OD). A thorough analysis of the imaginary part of the impedance is required in order to get a good dielectric characterization for each measurement. In Fig. 3a–c we present the imaginary part of the measured (uncorrected) impedance of cell suspension, Im[$Z$] (full circles); the impedance of the medium or supernatant, Im[$Z_m$] (solid line); the polarization impedance, Im[$Z_p$] (dashed line); and finally the corrected or the intrinsic impedance of the cell suspension for three concentrations (ODs) obtained after polarization removal, Im[$Z_s$] (open circles). As one can see, Im[$Z_p$] becomes negligible starting at 10 kHz for each cell suspension. In other experimental trials (not shown here), if the cells were not centrifuged gently, the conductivity of the supernatant became much larger than the conductivity of the cell suspension due to cell lysis. This conductivity issue is directly seen as an increase in Im[$Z$] of the supernatant. In other words, the conductivity of the cells and collected supernatant must be very carefully monitored and their values should be similar.

The polarization effect increased the relative dielectric permittivity of the suspension at 10 Hz by approximately half of an order of magnitude on average. The inset in Fig. 3b shows a magnification of the plots and reveals that that Im[Z] of cells is significantly different from Im[$Z_m$] of the supernatant. Conductivity of the supernatant was also measured at 25°C with a conductivity meter (Denver Instrument 220). The measured and the fitted conductivities are in agreement to the first significant digit. The fitting parameters $\varepsilon$ and $\sigma$ for the medium are presented in Table 1, along with the measured conductivity of the supernatant.

The intrinsic relative dielectric permittivity for the three suspensions with different *E. coli* concentrations is plotted in Fig. 3d. At low frequencies, the relative dielectric permittivity is increasing as the concentration of cells is

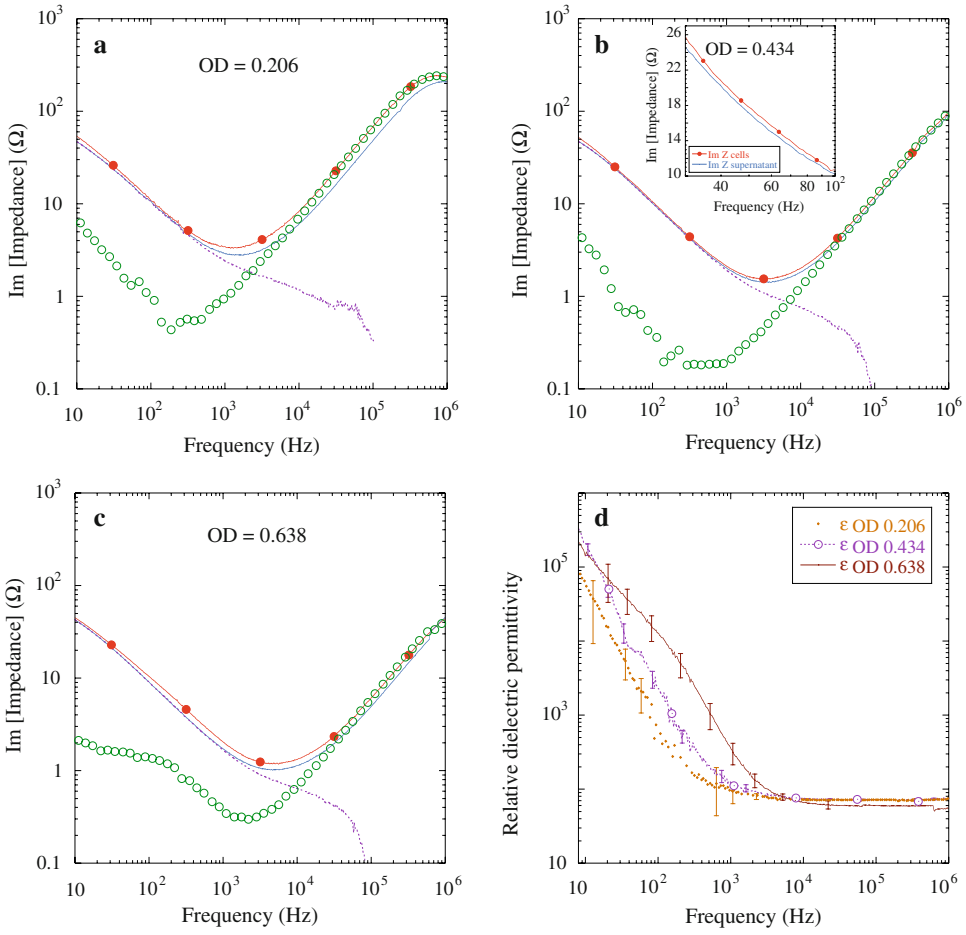


**Fig. 3** **a–c** Imaginary parts of impedances: cell suspension (Im[Z], *red*, *circles*), supernatant (Im[$Z_m$], *blue*, *solid line*), polarization error (Im[$Z_p$], *purple*, *dashed line*) and corrected cells after polarization removal (Im[$Z_s$], *green*, *empty circles*) plotted as a function of frequency. **d** Corrected relative dielectric permittivity for the three suspensions with different *E. coli* concentrations: OD 0.206 (*orange*, *dotted line*), 0.434 (*purple*, *empty circles*), and 0.638 (*brown*, *solid line*)

**Table 1** The fitting parameters $\varepsilon$ and $\sigma$ of the suspension medium for different ODs of the cells

| OD | $\varepsilon$ Fitted | $\varepsilon$ Fitted std error | $\sigma$ Fitted (S/m) | $\sigma$ Fitted std error | $\sigma$ Measured (S/m) at 25.8°C | $R$ |
|---|---|---|---|---|---|---|
| 0.206 | 72.56 | 0.26 | $3.08 \times 10^{-3}$ | $6.82 \times 10^{-6}$ | $3.09 \times 10^{-3}$ | 0.99 |
| 0.434 | 70.71 | 0.16 | $5.74 \times 10^{-3}$ | $2.77 \times 10^{-6}$ | $5.41 \times 10^{-3}$ | 0.99 |
| 0.638 | 67.12 | 0.23 | $9.75 \times 10^{-3}$ | $3.17 \times 10^{-6}$ | $9.29 \times 10^{-3}$ | 0.99 |

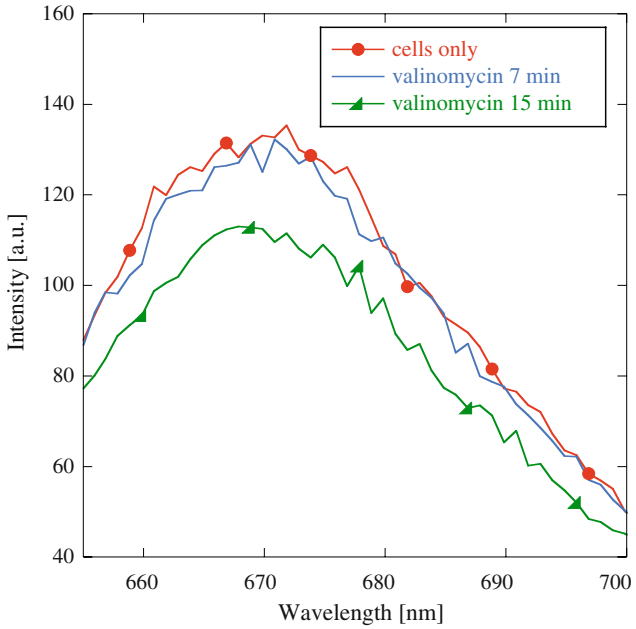


**Fig. 4** Fluorescence intensity versus wavelength for cells in water: cells only (*red*, *circles*), cells after 7 min of valinomycin addition (*blue*, *solid line*), cells after 15 min of valinomycin addition (*green*, *triangles*)

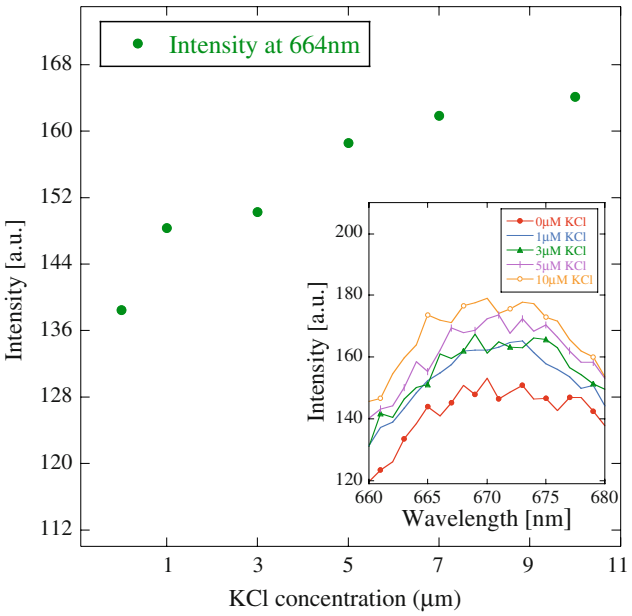


**Fig. 5** Fluorescence intensity plotted at 664 nm with the addition of KCl to the suspension of cells. *Inset* presents raw data for the fluorescence quenching as a function of wavelength. As KCl is added to the solution of cells labeled with voltage-sensitive dye, the fluorescence intensity of the dye increases. Changes in fluorescence were previously correlated with changes in the membrane potential (0.5% change in intensity corresponds to 1 mV change in the membrane potential of the dye, see text)

increased (correlated with OD). The intrinsic relative dielectric permittivity for OD 0.434 has values on the order of $6.5 \times 10^5$ at low frequency and the values are decreasing towards 70 at high frequencies. The intrinsic relative dielectric permittivity for OD 0.638 has the highest value equal to $7.9 \times 10^5$, which occurs at low frequencies, and the values are decreasing towards 67 at high frequencies. As OD increases, the conductivity of the cell suspension (and collected supernatant) also increases due to a larger depletion of salts as metabolites. Thus, the electrode polarization error increases with the increase in the cell concentration.

We now move on to the experiments in which we induced variations in the membrane potential. These variations were induced using KCl and in the presence of valinomycin. During the early logarithmic phase of growth, the intracellular K concentration in *E. coli* exceeds that of the external medium (Schultz and Solomon 1961). When valinomycin was added to the suspension, the cells membranes were made permeable to the $K^+$ ions inside the cells and a flow started due to unhindered diffusion. Since $K^+$ is more concentrated inside the cells, the net movement of the charges is from inside out, down the concentration gradient, until an equilibrium membrane potential is reached. This is a common mechanism by which many cells re-establish a membrane potential.

In Fig. 4, the effect of valinomycin on the cellular membrane potential was probed using voltage-sensitive dyes. Again, we see a decrease in the fluorescence intensity after 20 min of adding valinomycin and it proves the effort of the cells to balance $\Delta V$. At some point, an equilibrium resting membrane potential is reached. Changing the potassium concentration outside the cells induced further variations in the resting membrane potential. This will change the potassium concentration gradient and a new resting potential will be established. This can be directly correlated to the fluorescence quenching of Di-SC3-5, which is classified as a slow-response probe with changes in intensity of 0.2–0.5% per mV change in membrane potential (Sims et al. 1974; Suzuki et al. 2003; Waggoner 1976). In Fig. 5 we present the fluorescence intensity after

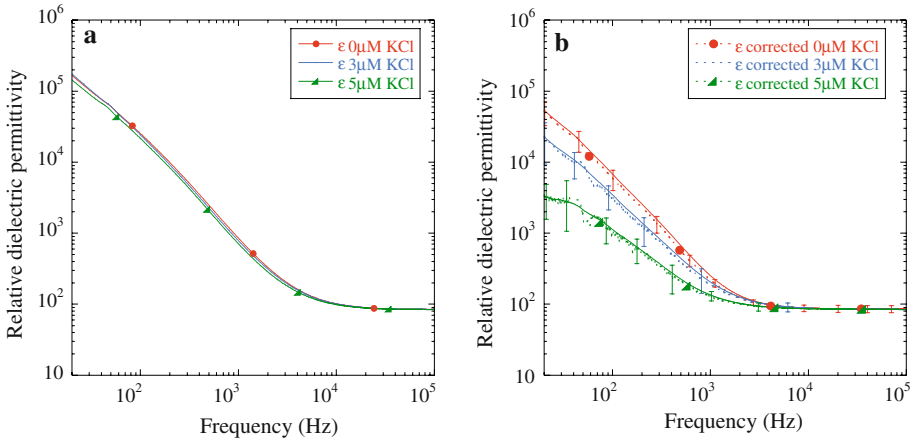


**Fig. 6** **a** Relative dielectric permittivity of *E. coli* and KCl concentrations (μM) (computed from the raw data). **b** Relative dielectric permittivity of *E. coli* and KCl concentrations (μM) after polarization removal. It can be seen here that as KCl is added to the solution with the cell suspension, the low-frequency dielectric permittivity decreases while the high-frequency dielectric permittivity (above 5,000 Hz) remains unchanged

**Table 2** The fitting parameters $\varepsilon$ and $\sigma$ of the suspension medium for membrane potential changes

| [KCl] | $\varepsilon$ Fitted | $\varepsilon$ Fitted std error | $\sigma$ Fitted | $\sigma$ Fitted std error | $R$ value |
|---|---|---|---|---|---|
| 0 μM | 69.15 | 0.22 | $3.69 \times 10^{-3}$ | $8.77 \times 10^{-8}$ | 0.99 |
| 3 μM | 66.74 | 0.32 | $4.01 \times 10^{-3}$ | $1.12 \times 10^{-7}$ | 0.98 |
| 5 μM | 68.01 | 0.26 | $3.61 \times 10^{-3}$ | $9.93 \times 10^{-8}$ | 0.99 |

the addition of KCl to the suspension of cells. The changes in intensity are proportional to a membrane depolarization and an increase in membrane potential. By calculating the percentage change in fluorescence as $\Delta F = 100(F_f - F_i)/F_i$ (Hoffman and Laris 1974) and using 0.5% per mV change (Suzuki et al. 2003), we obtained an average of 10-mV membrane potential increase correlated to $\Delta F$. In the inset in Fig. 5, the raw data for the fluorescence quenching are presented as a function of wavelength.

In order to probe these changes in $\Delta V$ using DS, we used suspensions of cells in pure water with 5 mM glucose under the same conditions as for fluorescence measurements. Each suspension was accommodated with 1 μM valinomycin, and after approximately 20 min, KCl was added externally. In Fig. 6a, the relative dielectric permittivity computed from the raw data is plotted for two KCl concentrations compared with cells only; these were chosen because they exhibited a more significant change in fluorescence (as in Fig. 5). After the polarization errors are removed as described before, we can easily distinguish between the curves corresponding to various KCl concentrations added (see Fig. 6b). In this latter figure, all the dispersion curves of the intrinsic relative dielectric permittivity are decreasing with increasing KCl concentration, in accordance with the theoretical model described in Prodan and Prodan (1999) and Prodan et al. (2008). Indeed, with the addition of KCl, the cell membrane depolarizes and, according to the theoretical models, one should observe a decrease in the low-frequency dielectric function. The fitted parameters for the supernatant are presented in Table 2. The error bars represent the standard deviation determined over four to five experiments for each dispersion curve. We should mention here that the supernatant impedances were measured separately for the different KCl concentrations added to the cell suspension.

## Discussion

Currently used techniques for sterilizing drinking water from coliforms or other bacteria-starvation assays (Cuny et al. 2005) start with resuspending the cells in Milli-Q water without any source of energy. *E. coli* cells are usually left to settle with or without shaking overnight before any sterilization tests (Liu 2005). This motivated our interest in having fully viable cells in Milli-Q water with 5 mM glucose and using them for measurements. Each measurement lasts less than 25 min, including the incubation time required by valinomycin.

In Fig. 3d, we indicate the changes in the relative dielectric permittivity related to cell concentration. The lowest concentration had the lowest values for $\varepsilon$, and the increase in the cell concentration is directly proportional to the increase in $\varepsilon$. The parameters listed in Tables 1 and 2 given by the fitting technique when removing the polarization effects have a low standard error for $\varepsilon$ (0.2) and even lower for $\sigma$ ($\sim 10^{-7}$). The fitting was done on values at frequencies higher than $10^4$ Hz. The experimental outcomes for the relative dielectric permittivity at high frequencies are in good agreement with the results presented by other authors, for example Mihai et al. (1996), who found values ranging from 70 to 74 for suspensions of ellipsoidal cells. For *E. coli* in culture medium, Ong et al. (2001) found $\varepsilon$ values ranging from 92 to 95 at 5 MHz and Bai et al. (2006) found roughly 100.

The second set of experiments indicates that DS can distinguish between suspensions of cells with different membrane potentials. In these experiments, the concentration of cells (OD) was kept the same; just the membrane potential was varied from one experiment to another. The membrane potential was changed in steps of 10 mV using KCl. Using images taken with the microscope, we concluded that the addition of the KCl did not change the shape or volume of the cells due to osmotic pressure.

Next, our experimental results for the dielectric permittivity are combined with the theoretical model. We present the application of the theoretical model from Prodan and Prodan (1999) to obtain the value of membrane potential from the DS measurements.

It was recently shown (Prodan et al. 2008) that this theoretical model has an analytical solution if the cells are considered spherical and as described under "Materials and methods". For simplicity, we will use this model and approximate *E. coli* cells with spherical cells as best we can. The input parameters for the model are the following: (1) the diffusion constant, $D$, of surface charges accumulated at the outer and inner surfaces of the membrane, which was adjusted to best fit the data, (2) the volume fraction, $p$, obtained based on microscope images of cells, (3) cell radius fixed at 1.5 μm, (4) $\varepsilon_1 = 40$ for cells without valinomycin (Fig. 3), and $\varepsilon_1 = 50$ for valinomycin-treated cells (Fig. 6), (5) $\varepsilon_0$ and $\sigma_0$ of the medium, the measured values listed in Tables 1 and 2, (6) $\varepsilon_2 = 78$ and $\sigma_2 = 0.2$ S/m (Bai et al. 2006), (7) thickness of the inner membrane, $d = 5$ nm (Matias et al. 2003). We want to comment on this latter choice. *E. coli* K12 are gram-negative bacteria and have two membranes separated by a cell wall in between. The inner membrane acts as the permeability barrier while the outer membrane and cell wall provide additional protection (Berg et al. 2002). The outer membrane is different from ordinary lipid bilayers and is not regarded as a barrier for ions but as a filter to exclude large molecules (Bai et al. 2006). Because of these properties, we chose only the inner membrane as the membrane that provides the ion separation. The last input parameter for the model is the membrane potential. Using the analytic model, we have simulated the experimental dielectric curves reported in Fig. 3d, as well as those reported in Fig. 6b. These simulations are presented in Fig. 7.

For the first set of data, the volume fractions considered were 0.015 for OD 0.206, 0.06 for OD 0.434, and 0.09 for OD 0.638. A resting membrane potential of −180 mV was kept the same for all three concentrations. We would like to comment on this value. Cells in media undergoing pH changes from acidic to alkaline normally have a resting membrane potential of −150 mV (Felle et al. 1980; Zilberstein et al. 1998). When cells are harvested from the growth medium and placed in water with 5 mM glucose, they hyperpolarize as shown in Fig. 4. Moreover, the addition of valinomycin hyperpolarizes the membrane by another 10 mV, over and beyond the hyperpolarization that cells undergo when they are re-suspended in water and glucose. Thus, using the fluorescence measurements, we estimated that the membrane potential of cells in water with 5 mM glucose would be around −180 mV. The results of this model for cell concentrations are presented in Fig. 7a, where the solid lines represent the theoretical curves and the dotted lines are the experimental results.

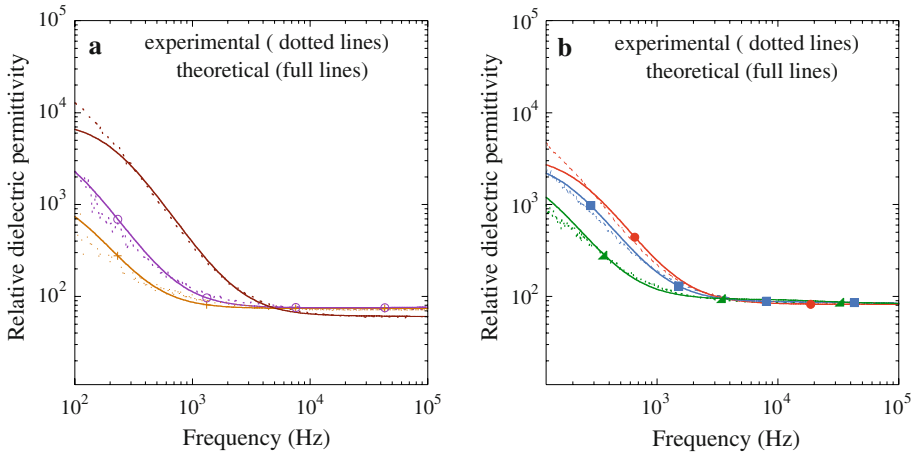


**Fig. 7** **a** Relative dielectric permittivity of *E. coli* for OD 0.206 (*orange*, *cross*), 0.434 (*purple*, *empty circles*), and 0.638 (*brown*, *solid line*) theoretical simulations (*solid lines*) and experimental results (*dotted lines*). As the cell concentration changes, the low and high dielectric permittivity changes, but the absolute value of the membrane potential remains the same (180 mV). The membrane potential was obtained by fitting the experimental curves with the theoretical model described in this paper. **b** Relative dielectric permittivity of *E. coli* for the following membrane potentials: −180 mV (*red*, *circles*), −170 mV (*blue*, *squares*), and −160 mV (*green*, *triangles*) theoretical simulations (*solid lines*) and experimental results (*dotted lines*)

For the second set of data presented in Fig. 6b, where we studied the effect of membrane potential variations, the simulation is shown Fig. 7b. The volume fraction for these suspensions was 0.02 (as obtained by direct imaging). The cytoplasm's conductivity was varied from 0.2 to 0.25 S/m because the conductivity inside the cells should increase with the addition of KCl. Membrane potential was varied by depolarization in 10 mV steps from −180 to −160 mV. In Fig. 7b, the solid lines represent the theoretical curves and the dotted lines are the experimental results.

The experimental data shown in Figs. 3 and 6 show one dispersion only. The question we will address next is which plateau, alpha or beta? From previous experiments (Bai et al. 2006), we know that *E. coli* suspensions can exhibit a beta dispersion in the kHz–MHz region. A significant difference between our measurements and theirs is that in the latter the cells were measured in the growth medium, which has a conductivity about 440 times higher than the water, which was the medium for our experiments. To see the effect of such a difference, we increased the conductivity of the medium from $6 \times 10^{-3}$ to $3 \times 10^{-2}$ S/m in our simulations, and we plotted the results in Fig. 8. In these theoretical simulations we used a volume fraction of 0.09 and a resting membrane potential of −180 mV; all other parameters were kept as before. For the curves shown in Fig. 8, the only parameter that was varied was the conductivity of the medium. One can observe, as the conductivity of the medium is increased, the beta plateau becomes more prominent and it extends in the region 10 kHz–1 MHz. With a conductivity of $3 \times 10^{-2}$ S/m, the beta dispersion starts to appear at 0.1 MHz, similar to the experiments of Bai et al. (2006) where beta dispersion appears at 0.2 MHz. Now we can be sure that the beta plateau is absent in our experimental data because the conductivity of the medium was very low. Moreover, our theoretical simulations further indicate that the plateau seen in our data represents the alpha plateau since there is a strong variation with the membrane potential. The tails of the dielectric curves come together in high frequency (starting 3 kHz) and have values close to the dielectric permittivity of water.

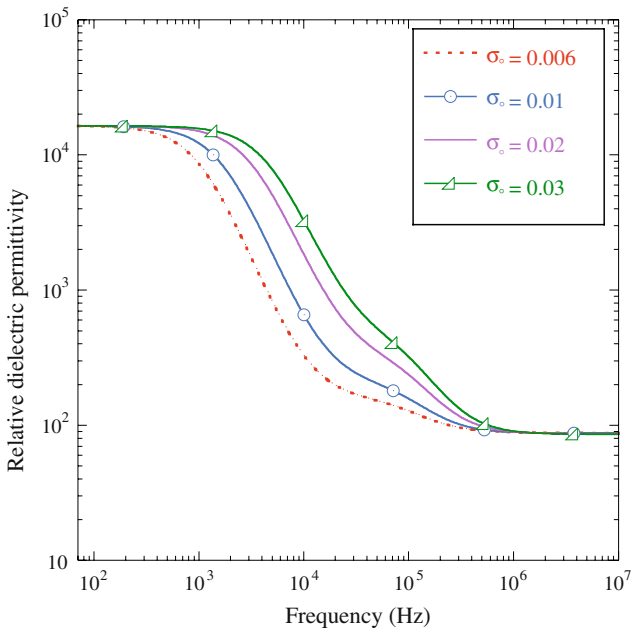


**Fig. 8** Relative dielectric permittivity of *E. coli* versus frequency: theoretical simulations for outside medium conductivity ($\sigma_0$) variations ($\sigma_0 = 0.006$ S/m *red*, *dotted line*; $\sigma_0 = 0.01$ S/m *blue*, *empty circles*; $\sigma_0 = 0.02$ S/m *purple*, *solid line*; $\sigma_0 = 0.03$ S/m *green*, *empty triangles*)

The first set of measurements, on cell suspension at different concentrations, indicates that DS can provide an effective way to distinguish between cell suspensions with different volume fractions and at the same membrane potential. Judging by the error bars, a minimum 4.5% change in the volume fraction can be detected. The second set of experiments, where different KCl concentrations are added to the cells in order to vary the membrane potential, suggests that changes of 10 mV or more in the membrane potential can be monitored with this technique.

Each experimental dielectric curve required about 5 min to record. Thus, changes that occurred within 5 min could not be monitored. However, this time could be reduced, if needed. The number of points in the data presented here are 500 for each experimental dielectric curve. Thus, by reducing the number of points, less time would be required for a measurement. For example, 100 points for the whole interval means a 33 point per frequency interval; this should be sufficient for a reliable measurement. With sufficient testing, the number of points can be further reduced to require maybe seconds in this frequency range.

We should also point out that the technique presented here works in for low cell concentrations. The polarization removal process will not work at large volume fractions where the presence of the cells can affect the electrode polarization impedance.

## Conclusions

In this paper we demonstrate a quantitative way to measure the membrane potential of living cells by dielectric spectroscopy. This method can be applied to any type of live cells in suspensions. To obtain the membrane potential, we fitted out experimental dispersion curves with the ones obtained from a theoretical model, with the membrane potential as the fitting parameter. We also show that the values of the membrane potential obtained using our technique are in good agreement with those obtained using traditional methods—voltage-sensitive dyes. To obtain the intrinsic dispersion curves for cell suspensions, the

polarization error was removed by using the method from Prodan and Bot (2009).

Electrical impedance measurements were made on a culture of *E. coli* cells in the frequency range of 10 Hz–1 MHz using a two-electrode system. First, the measurements made on three different concentrations of cells in suspensions using this technique show that the increase in dielectric permittivity after polarization removal is proportional to changes in optical density, thus to the concentration of cells. In the alpha-frequency domain, the lowest concentration of cells in the suspension had the lowest values for $\varepsilon$, and an increase in cell concentration is directly proportional to an increase in $\varepsilon$. In the high-frequency domain (10 kHz and up), the relative dielectric permittivity is close to that of the suspending medium and the values are in the range of 67–72 for various cells concentrations. Second, we presented the relationship between membrane potential variations and dielectric permittivity in the low-frequency range. Experimentally, the membrane potential was changed using different concentrations of KCl in the presence of valinomycin. KCl depolarizes the cell membrane, and this was observed as a direct decrease in the low-frequency dielectric constant (alpha relaxation) for each KCl concentration considered. By using the theoretical model presented in Prodan and Prodan (1999) and Prodan et al. (2008), we extracted the membrane potential for each KCl concentration. Conductivity of the supernatant needs to be closely monitored, as it plays a major role in removing the polarization error (i.e., if the cells are centrifuged gently, the conductivity of the supernatant is not unnecessarily increased due to cell lysis).

In conclusion, we presented a method here to obtain and monitor the membrane potential by dielectric spectroscopy that is noninvasive and label free. This method could be used for fundamental research in life sciences as well as developed into a high throughput screening for pharmaceutical agents.

**Acknowledgments** This work was supported, in part, by the grant NJIT-ADVANCE awarded by the National Science Foundation (grant no. 0547427).

## References

Asami K, Gheorghiu E, Yonezawa T (1999) Real-time monitoring of yeast cell division by dielectric spectroscopy. Biophys J 76:3345–3348

Bai W, Zhao KS, Asami K (2006) Dielectric properties of *E. coli* cell as simulated by the three-shell spheroidal model. Biophys Chem 122:136–142

Bai W, Zhao K, Asami K (2007) Effects of copper on dielectric properties of *E. coli* cells. Colloids Surf B Biointerfaces 58:105–115

Berg JM, Tymoczko JL, Stryer L (2002) Biochemistry, 5th edn. WH Freeman, New York

Bordi F, Cametti C, Gili T (2001) Reduction of the contribution of electrode polarization effects in the radiowave dielectric measurements of highly conductive biological cell suspensions. Bioelectrochemistry 54:53–61

Ciureanu M, Levadoux W, Goldstein S (1997) Electrical impedance studies on a culture of a newly discovered strain of *Streptomyces*. Enzyme Microb Technol 21:441–449

Cuny C, Dukan L, Fraysse L, Ballesteros M, Dukan S (2005) Investigation of the first events leading to loss of culturability during *Escherichia coli* starvation: future nonculturable bacteria form a subpopulation. J Bacteriol 187:2244–2248

Felle H, Porter JS, Slayman CL, Kaback HR (1980) Quantitative measurements of membrane potential in *Escherichia coli*. Biochemistry 19:3585–3590

Hoffman JF, Laris PC (1974) Determination of membrane potentials in human and *Amphiuma* red blood cells by means of a fluorescent probe. J Physiol 239:519–552

Keese CR, Wegener J, Walker SR, Giaever I (2004) Electrical wound-healing assay for cells in vitro. Proc Natl Acad Sci USA 101:1554–1559

Leung G, Tang HR, McGuinness R, Verdonk E (2005) Cellular dielectric spectroscopy: a label-free technology for drug discovery. J Assoc Lab Autom 10:258–269

Liu G (2005) An investigation of UV disinfection performance under the influence of turbidity and particulates for drinking water applications. M.Sc. Thesis, University of Waterloo

Mates SM, Eisenberg ES, Mandel LJ (1982) Membrane potential and gentamicin uptake in *Staphylococcus aureus*. Proc Natl Acad Sci USA 79:6693–6697

Matias VRF, Al-Amoudi A, Dubochet J, Beveridge TJ (2003) Cryotransmission electron microscopy of frozen-hydrated sections of *Escherichia coli* and *Pseudomonas aeruginosa*. J Bacteriol 185:6112–6118

Mihai CM, Mehedintu M, Gheorghiu E (1996) The derivation of cellular properties from dielectric spectroscopy data. Bioelectrochem Bioenerg 40:187–192

Morita S, Umakoshi H, Kuboi R (2000) Dielectric response of cells and liposomes and its utilization for evaluation of cell membrane–protein interaction. J Biosci Bioeng 90:157–162

Ong KG, Wang J, Singh RS, Bachas LG, Grimes CA (2001) Monitoring of bacteria growth using a wireless, remote query resonant-circuit sensor: application to environmental sensing. Biosens Bioelectron 16:305–312

Prodan C, Bot C (2009) Correcting the polarization effect in the very low frequency dielectric spectroscopy. http://arxiv.org/ftp/arxiv/papers/0805/0805.1648.pdf. Accessed 24 June 2009

Prodan C, Prodan E (1999) The dielectric behavior of living cell suspensions. J Phys D Appl Phys 32:335–343

Prodan C, Mayo F, Claycomb JR, Miller JH Jr (2004) Low-frequency, low-field dielectric spectroscopy of living cell suspensions. J Appl Phys 95:3754–3756

Prodan E, Prodan C, Miller JH (2008) The dielectric response of spherical live cells in suspension: an analytic solution. Biophys J 95:4174–4182

Raicu V, Saibara T, Irimajiri A (1998) Dielectric properties of rat liver in vivo: a noninvasive approach using an open-ended coaxial probe at audio/radio frequencies. Bioelectrochem Bioenerg 47:325–332

Ron A, Singh R, Fishelson N, Shur I, Socher R, Benayahu D, Shacham-Diamand Y (2008) Cell-based screening for membranal and cytoplasmatic markers using dielectric spectroscopy. Biophys Chem 135:59–68

Schultz SG, Solomon AK (1961) Cation transport in *Escherichia coli*: I. Intracellular Na and K concentrations and net cation movement. J Gen Physiol 45:355–369

Schwan HP (1968) Four-electrode null techniques for impedance measurement with high resolution. Rev Sci Instrum 39:481

Sims J, Waggoner AS, Wang CH, Hoffman JF (1974) Studies on the mechanism by which cyanine dyes measure membrane potential in red blood cells and phosphatidylcholine. Vesicles Biochem 16:3315–3330

Sohn LL, Saleh OA, Facer GR, Beavis AJ, Allan RS, Notterman DA (2000) Capacitance cytometry: measuring biological cells one by one. Proc Natl Acad Sci USA 97:10687–10690

Suzuki H, Wang Z, Yamakoshi M, Kobayashi M, Nozawa T (2003) Probing the transmembrane potential of bacterial cells by voltage-sensitive dyes. Anal Sci 19:1239–1242

Waggoner AS (1976) Optical probes of membrane potential. J Membr Biol 27:317–334

Wright S (2004) Generation of resting membrane potential. Adv Physiol Educ 28:139–142

Wu M, Maier E, Benz R, Hancock REW (1999) Mechanism of interaction of different classes of cationic antimicrobial peptides with planar bilayers and with the cytoplasmic membrane of *Escherichia coli*. Biochemistry 38:7235–7242

Yang L, Li Y (2006) Detection of viable *Salmonella* using microelectrode-based capacitance measurement coupled with immunomagnetic separation. J Microbiol Methods 64:9–16

Zhivkov AM, Gyurova AY (2008) High frequency electric polarizability of bacteria *E. coli*: dependence on the medium ionic strength. Colloids Surf B Biointerfaces 66:201–205

Zilberstein D, Agmon V, Schuldiner S, Padan E (1998) *Escherichia coli* intracellular pH, membrane potential, and cell growth. J Bacteriol 158:246–252